

# Analytic expressions for atomic layer deposition: Coverage, throughput, and materials utilization in cross-flow, particle coating, and spatial atomic layer deposition

Angel Yanguas-Gil and Jeffrey W. Elam<sup>a)</sup>

Argonne National Laboratory, Energy Systems Division, 9700 S Cass Ave, Lemont, Illinois 60439

(Received 20 September 2013; accepted 21 February 2014; published 12 March 2014)

In this work, the authors present analytic models for atomic layer deposition (ALD) in three common experimental configurations: cross-flow, particle coating, and spatial ALD. These models, based on the plug-flow and well-mixed approximations, allow us to determine the minimum dose times and materials utilization for all three configurations. A comparison between the three models shows that throughput and precursor utilization can each be expressed by universal equations, in which the particularity of the experimental system is contained in a single parameter related to the residence time of the precursor in the reactor. For the case of cross-flow reactors, the authors show how simple analytic expressions for the reactor saturation profiles agree well with experimental results. Consequently, the analytic model can be used to extract information about the ALD surface chemistry (e.g., the reaction probability) by comparing the analytic and experimental saturation profiles, providing a useful tool for characterizing new and existing ALD processes. © 2014 American Vacuum Society. [<http://dx.doi.org/10.1116/1.4867441>]

## I. INTRODUCTION

In recent years, the range of potential applications for atomic layer deposition (ALD) has expanded beyond semiconductor manufacturing into areas such as catalysis, energy storage, and photovoltaics.<sup>1–6</sup> One of the chief advantages of ALD is that it is intrinsically scalable. In fact, the same self-limited nature that allows conformal coating of high aspect ratio features makes it possible to coat arbitrarily large substrates and facilitates the transition from lab to industry. However, the viability of ALD for large-scale manufacturing in these new areas will be dictated by practical considerations such as throughput and precursor utilization.

In an effort to bring these new applications to fruition, three strategies are being pursued for high speed, high efficiency ALD: cross-flow reactors, spatial ALD, and particle coating.<sup>7–9</sup> One common challenge cutting across these three strategies is that, while new ALD processes are constantly being developed, there is no simple way to calculate the throughput or precursor utilization based on the deposition parameters and the ALD chemistry. While this does not stop the development of ever more efficient processes, it obfuscates direct comparisons with competing strategies for materials synthesis such as chemical vapor deposition and sputtering. Curiously enough, there has been a strong interest in understanding the dynamics of coating high-aspect ratio structures at the feature scale in ALD.<sup>10–13</sup> However, this interest has so far not carried through to the reactor scale, where simulation efforts have always been oriented to the numerical solution of transport equations or the use of computational fluid dynamic approaches and multiscale models.<sup>14–18</sup> Likewise, there is a strong research effort directed toward predicting ALD reaction kinetics from first principles calculations.<sup>19–21</sup> Combining computational fluid dynamics

with these first principles calculations offers the potential to further our understanding of the interplay between atomistic aspects of surface kinetics and the performance of an ALD process at a reactor scale. However, these simulations are very system-specific. An alternative approach, widely applied in the field of chemical vapor deposition (CVD), is the use of simpler kinetic models from which it is possible to extract effective kinetic data by fitting growth rates and growth profiles as a function of the experimental conditions.<sup>22–24</sup> These models help rationalize the results obtained and can be used to extract effective values of lumped kinetic data, evaluate the ideality of different processes, and more importantly, extrapolate the behavior of a system to scale-up conditions. However, the time dependent nature of ALD makes the derivation of analytic expressions more difficult compared with the conventional steady-state conditions in CVD.

The purpose of our work is to fill this gap by providing models for coverage, throughput, and materials utilization in the three main ALD manufacturing strategies: cross-flow, particle coating, and spatial ALD. Rather than focusing on detailed numerical models, our approach uses simple yet correct models that can be solved analytically and that lead to closed expressions in which the impact of each parameter can be easily identified. In the case of cross-flow reactors, we validate our model by direct comparison with experimental growth profiles. Our results show that, despite the differences in equipment and mode of operation, a universal expression for throughput and materials utilization can be obtained for all these systems, in which the characteristics of the reactor are contained in a single parameter. This expression is also coincident with the analytic expressions previously derived for ALD under diffusive transport for coating high aspect ratio features and nanostructured substrates.<sup>12,25</sup> This highlights the fact that, despite the wide variability in designs, the underlying physics controlling throughput and materials utilization is the same in all cases.

<sup>a)</sup>Electronic mail: [jelam@anl.gov](mailto:jelam@anl.gov)

## II. MODEL AND RESULTS

### A. ALD surface chemistry

We have modeled the ALD surface chemistry using an irreversible, first-order Langmuir kinetic model, which has been extensively used in the literature.<sup>10,14,15</sup> In this approximation, the change in the fraction of available sites  $\theta$ , which is related to the surface coverage or reacted precursor molecules through  $c = 1 - \theta$ , is first order in both  $\theta$  and the precursor gas density  $n$ .  $n$  is related to the precursor partial pressure through the ideal gas equation:  $p = nk_B T$ .

$$\frac{\partial \theta}{\partial t} = -s_0 \frac{1}{4} v_{th} \beta_0 \theta n. \quad (1)$$

Here,  $v_{th}$  the mean thermal velocity,  $s_0$  is the average area of a surface site, which is related to the growth per cycle or, more directly, to the net mass gain as measured using a quartz crystal microbalance. Finally,  $\beta_0$  is the bare reaction probability, which is the probability that an incident precursor molecule reacts on a pristine surface. Using this model, the surface chemistry is represented by just two parameters:  $\beta_0$  and  $s_0$ .

### B. Cross-flow reactor

Simple 1-D models of cross flow reactors based on the self-limited ALD model described above have been

presented in the literature with and without axial diffusion (plug flow), and in both cases, good agreement with experiment was obtained.<sup>14,15</sup> Likewise, an equivalent discrete model of a plug flow reactor has been used by Knoops.<sup>26</sup> However, all these precedents rely on a numerical solution of the corresponding equations, which makes it hard to extract analytic expressions for throughput and materials utilization.

Here, we will consider a plug flow model in which the density of species along a reactor is given by the equation

$$\frac{\partial n}{\partial t} + u \frac{\partial n}{\partial z} = -\frac{S}{V} \frac{1}{4} v_{th} \beta_0 \theta n. \quad (2)$$

Here,  $S$  is the reactor surface area,  $V$  is the reactor volume, and  $u$  is the axial flow velocity. This is essentially the model considered by Ylilammi and later by Yanguas-Gil but setting axial diffusion to zero.<sup>14,15</sup> This equation, along with Eq. (1), is subject to the following initial and boundary conditions: the process is characterized by a profile of the available sites at the beginning of the pulse  $\theta(z, 0)$ , and a density profile at the entrance of the reactor  $n(0, t)$ . The density profile at the inlet represents the pressure profile during the precursor dose, which in our model can take any arbitrary shape.

It can be shown that Eqs. (1) and (2) subject to the initial and boundary condition described above can be solved analytically, resulting in

$$c(z) = 1 - \frac{\theta(z, 0) \exp\left(\frac{S}{Vu} \frac{1}{4} v_{th} \beta_0 \int_0^z \theta(z', 0) dz'\right)}{\exp\left(\frac{S}{Vu} \frac{1}{4} v_{th} \beta_0 \int_0^z \theta(z', 0) dz'\right) + \exp\left(s_0 \frac{1}{4} v_{th} \beta_0 \int_0^t n(0, t') dt'\right) - 1}. \quad (3)$$

This solution can be simplified for the case of a saturated surface  $\theta(z, 0) = 1$  so that the coverage profile in the reactor is given by

$$c(z) = \frac{\exp\left(s_0 \frac{1}{4} v_{th} \beta_0 \int_0^t n(0, t') dt'\right) - 1}{\exp\left(\frac{S}{Vu} \frac{1}{4} v_{th} \beta_0 z\right) + \exp\left(s_0 \frac{1}{4} v_{th} \beta_0 \int_0^t n(0, t') dt'\right) - 1}. \quad (4)$$

Equation (4) provides the coverage profile in a cross flow reactor as a function of the dose time. A key property of this solution is that it does not depend on the shape of the precursor pressure pulse but only on the total exposure. Therefore, using the average density and the dose time so that

$$t_d \bar{n} = \int_0^{t_d} n(0, t') dt'. \quad (5)$$

We finally obtain

$$c(z, t_d) = \frac{\exp\left(s_0 \frac{1}{4} v_{th} \beta_0 \bar{n} t_d\right) - 1}{\exp\left(\frac{S}{Vu} \frac{1}{4} v_{th} \beta_0 z\right) + \exp\left(s_0 \frac{1}{4} v_{th} \beta_0 \bar{n} t_d\right) - 1} = \frac{\exp(t_d/\bar{t}) - 1}{\exp(z/\bar{z}) + \exp(t_d/\bar{t}) - 1}. \quad (6)$$

Equation (6) depends of two parameters, a characteristic length  $\bar{z}$  and a characteristic time  $\bar{t}$ .

Equation (6) provides the surface coverage and the corresponding growth per cycle of the ALD process when the precursor dose is carried out under saturated conditions for the other reactants in the ALD process. These conditions are typically used when measuring uptake/saturation curves. In the most general case, a set of Eq. (3)—one for each step of the ALD cycle—needs to be solved self-consistently to extract

the final growth per cycle. Details on the model extension to treat the case of more than one precursor are shown in the Discussion.

Despite its simplicity, Eq. (6) is able to reproduce the experimental saturation profiles in tubular viscous-flow reactors. In a previous work, we carried out measurements of saturation profiles of trimethylaluminum (TMA) and water for different subsaturating TMA exposures.<sup>15</sup> In Fig. 1(a), we show a comparison between the experimental data (solid symbols) and the profiles determined using Eq. (6) (lines). To obtain the analytic profiles, we assumed a reaction probability of  $10^{-2}$ .<sup>13</sup> As a comparison, the corresponding curves for a reaction probability of  $10^{-3}$  are shown in Fig. 1(b). It is evident that, despite the simplicity of the model, Eq. (1) accurately predicts the coating profiles of ALD systems driven by a surface chemistry that is close to that of Eq. (6).

We can use Eq. (6) to determine the exposure time,  $t_d$  required to coat a reactor of a length  $L$ , and therefore the throughput of a process under scale up. By assuming that a saturation coverage  $c$  is obtained at  $z = L$ , we can express the throughput as

$$t_d = t_0 + \frac{S}{\bar{n}s_0V} \frac{L}{u}, \quad (7)$$

where  $t_0$  is the time required to achieve the saturation coverage  $c_0$  at the inlet, which can be determined either experimentally or analytically from

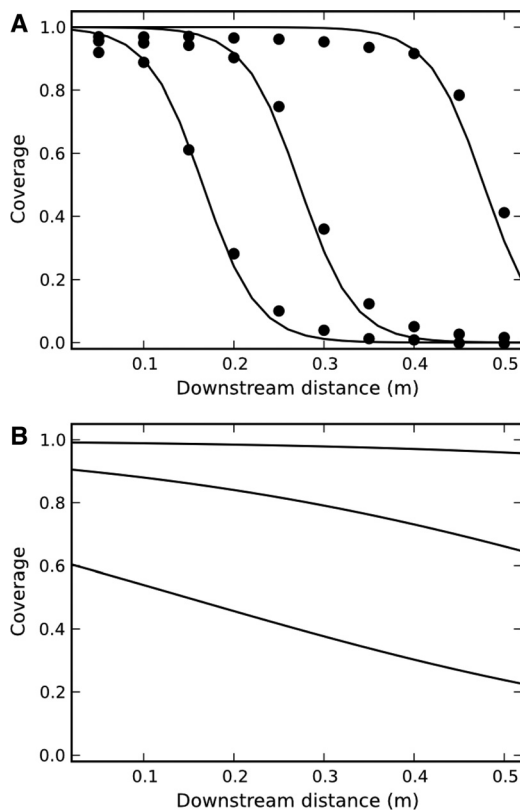


FIG. 1. (a) Comparison between growth profiles predicted by the analytic model for a reaction probability of  $10^{-2}$  based on Eq. (6) (lines) and experimental data obtained for increasing TMA dose times (symbols). (b) Growth profiles predicted by the analytic model for a reaction probability of  $10^{-3}$ .

$$t_0 = -\frac{4}{s_0\beta_0v_{th}\bar{n}} \ln(1-c). \quad (8)$$

According to Eq. (7), the time required to coat a reactor is the sum of a size-independent contribution (the saturation time) and a second term that is linear with the reactor length,  $L$ . This means that if  $t_0$  is sufficiently long (for instance, due to a low reaction probability), essentially no additional time is required to coat a larger substrate. Likewise, Eq. (7) shows that a higher flow velocity,  $u$  will reduce the additional time needed to coat large substrates. The  $S/V$  ratio, which is given by  $S/V = 1/(2d)$  for a parallel plate reactor with plate spacing  $d$ , and  $S/V = 1/(2R)$  for a tubular reactor with radius  $R$ , also affects the dependence of the dose time with size. Figure 2(a) shows how these two terms compete with each other. We show the predicted dose times normalized to the saturation time as a function of reactor size for four different values of the bare reaction probability [Fig. 2(a)] for a reactor with a radius or plate spacing of 2 cm, a flow velocity of 1 m/s and a precursor mass of 150 amu. The normalized times are independent of the precursor density  $\bar{n}$ , and the surface site area  $s_0$ . Lower reaction probabilities lead to lower throughputs;

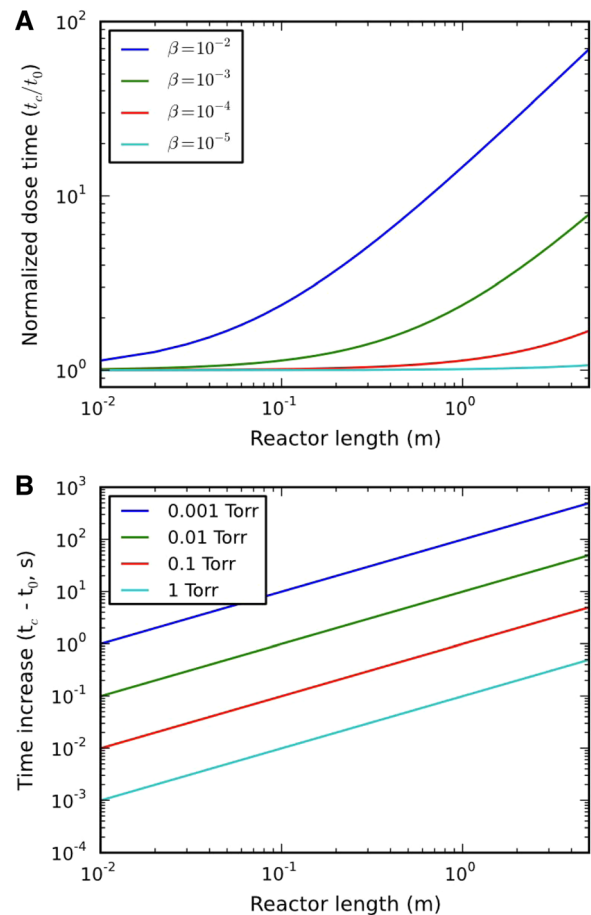


FIG. 2. (Color online) Results from the analytic model for a cross-flow reactor based on Eq. (6). (a) Impact of reactor size and reaction probability on the precursor dose time normalized to the saturation time at the inlet. (b) Impact of reactor size and precursor vapor pressure on the precursor dose time. Note that for precursor vapor pressures of  $\sim 0.001$  Torr and a reactor size greater than  $\sim 1$  m, the dose time increment exceeds 100 s.

however, in these systems, the throughput is relatively insensitive to reactor size. The actual time increases due to larger reactor sizes are shown in Fig. 2(b) for  $s_0 = 5 \text{ \AA}^2$  for the same geometry as Fig. 2(a). It is clear that high vapor pressure precursors are crucial to achieve a high throughput. A direct examination of Eq. (7) shows that this time increment is independent of the reaction probability.

By dividing the amount of precursor consumed by the total precursor exposure given by Eq. (7), we can calculate the precursor utilization  $\eta$ , the fraction of ALD precursor that is actually incorporated in the film

$$\eta = \frac{1}{1 + \frac{V \bar{n} s_0 u}{S L} t_0}. \quad (9)$$

Using the expression for  $t_0$  in Eq. (8), the precursor efficiency is found to be an increasing function of the following non-dimensional variable valid for both a parallel plate and a tubular reactor:

$$\eta = f\left(\beta_0 \frac{L v_{th}}{d u}\right). \quad (10)$$

Figure 3 shows some characteristic curves of Eq. (9) obtained for 99% coverage as a function of reaction probability at selected reactor sizes. One of the consequences of Eq. (10) is that the materials utilization is larger when the reaction probability increases. It is also interesting to note that the precursor utilization increases with scale up.

### C. Particle coating

We can apply the same procedure carried out in the previous section to determine the throughput and materials utilization for ALD particle coating under conditions typical of fluidized bed and rotating drum coating system. As with the cross-flow reactor, analytic solutions can be obtained under the well-mixed reactor approximation commonly used in chemical engineering.<sup>27</sup>

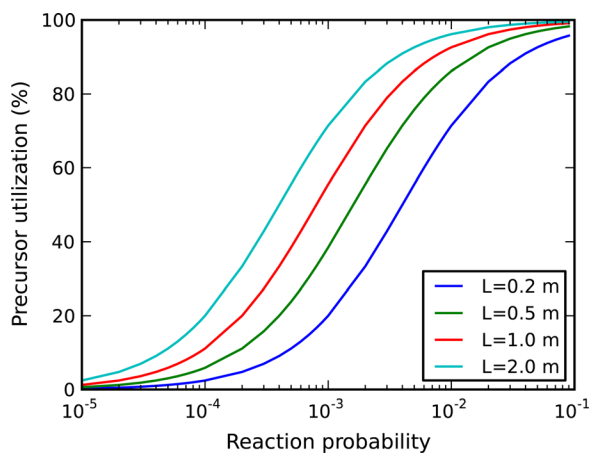


Fig. 3. (Color online) Impact of reaction probability and reactor size on precursor utilization predicted by the analytic model for a cross-flow reactor [Eq. (9)].

As shown in Fig. 4, the well-mixed approximation for particle coating assumes that a certain volumetric flow  $\phi_0$  of precursor is constantly being introduced at an inlet density  $n_0$  into a reactor of volume  $V$  containing a total surface area  $S$ . The total reactor pressure is kept constant by pumping or venting the mixture with the same volumetric flow as it is inserted. Under the well-mixed approximation, we assume that the density and coverage are homogeneous inside the reactor, and therefore only a function of time. Assuming a fast equilibration of the precursor density inside the reactor, we obtain the following two equations for the gas density of precursor molecules and the surface coverage:

$$\phi_0(n_0 - n) = S\beta_0 \frac{1}{4} v_{th} n \theta, \quad (11)$$

$$\frac{dc}{dt} = s_0 \beta_0 \frac{1}{4} v_{th} n (1 - c), \quad (12)$$

subject to the initial condition:  $c(0) = 0$  for a pristine surface.

From the solution to these equations, we can determine the time required to achieve a certain surface coverage  $c$

$$t_c = \frac{S}{\phi_0 s_0 n_0} - \frac{4}{v_{th} s_0 \beta_0 n_0} \ln(1 - c) = t_0 + \frac{S}{\phi_0 s_0 n_0}, \quad (13)$$

wherein by analogy to Eq. (8), we have defined  $t_0$  as

$$t_0 = -\frac{4}{s_0 \beta_0 v_{th} n_0} \ln(1 - c). \quad (14)$$

And, as in the case of the plug flow reactor, we have that the precursor utilization is given by

$$\eta = \frac{cS/s_0}{\phi_0 n_0 t_c}. \quad (15)$$

This is simply the ratio between the molecules consumed and the molecules dosed into the system. Substituting the expression for  $t_c$  in Eq. (13), we obtain that when  $c \rightarrow 1$

$$\eta = \frac{1}{1 - \frac{4\phi_0}{v_{th}\beta_0 S} \ln(1 - c)}. \quad (16)$$

Two important consequences of this equation are that the precursor utilization increases with the surface area, thereby

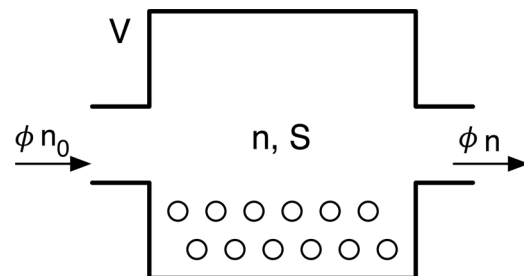


Fig. 4. Scheme for the ALD particle coating model under the well-mixed reactor approximation.

becoming more efficient, and that low volumetric flows are essential in order to achieve high materials utilization. The prefactor in Eq. (16) can be understood as the ratio between the volume of precursor molecules reaching the surface to the volume leaving the reactor. Note that the efficiency does not depend on the precursor density or the surface site area. As in the case of cross-flow reactors, the reaction probability plays an important role in determining the overall materials utilization through its effect in the dose time  $t_c$ .

#### D. Spatial ALD

A similar model can be applied to the case of spatial ALD as it is currently being implemented for roll-to-roll coating and continuous processing.<sup>7,28</sup> As shown in Fig. 5, we assume that the precursor is contained inside a chamber of volume  $V$ , and that a moving web (or substrate) with velocity  $u$  is exposed to the precursor over a length  $L$ . Under the well-mixed approximation, we assume that the moving web is exposed to a constant precursor density  $n$ , and that the precursor is injected into the chamber at a volumetric flow  $\phi_0$  and density  $n_0$ . As a particular surface site moves along with the web, its coverage increases according to the expression

$$u \frac{dc}{dz} = s_0 \beta_0 \frac{1}{4} v_{th} n (1 - c). \quad (17)$$

Assuming that all sites are uncoated as the web enters the chamber,  $c(0) = 0$ , we have

$$c(z) = 1 - \theta(z) = 1 - \exp\left(-\frac{s_0 \beta_0 v_{th} n z}{4u}\right). \quad (18)$$

And the average reaction probability  $\bar{\beta}$  inside the chamber is given by

$$\begin{aligned} \bar{\beta} L &= \beta_0 \int_0^L \theta(z) dz = \frac{4u}{s_0 v_{th} n} \left[ 1 - \exp\left(-\frac{s_0 \beta_0 v_{th} n L}{4u}\right) \right] \\ &= \frac{4u}{s_0 v_{th} n} c, \end{aligned} \quad (19)$$

where  $c$  is the final coverage achieved by a single pass through the chamber. Using Eq. (19) and an analogous expression to Eq. (11), we obtain the following expression for the average precursor density inside the chamber under the well-mixed approximation:

$$\phi_0 (n_0 - n) = S \bar{\beta} \frac{1}{4} v_{th} n = \frac{S u}{L s_0} c = \frac{S}{s_0} c \frac{1}{t_c}, \quad (20)$$

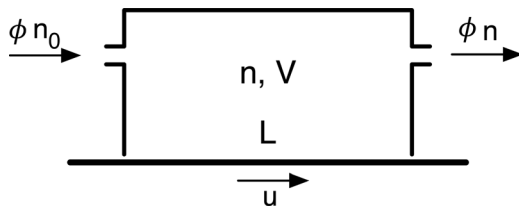


FIG. 5. Scheme for the spatial ALD model under the well-mixed reactor approximation. The moving web sees a constant precursor pressure as it moves along the chamber.

where we have defined the time  $t_c$  as the time a surface site in the web is exposed to the precursor  $t_c = L/u$ . From Eqs. (19) and (20) we can extract the residence time required to achieve a final coverage  $c$ , resulting in the expression:

$$t_c = \frac{L}{u} = \frac{S}{\phi n_0 s_0} - \frac{4}{\beta_0 s_0 v_{th} n_0} \ln(1 - c) = \frac{S}{\phi_0 n_0 s_0} + t_0, \quad (21)$$

where  $t_0$  is defined as in Eq. (14). Note that Eq. (21) is the same as Eq. (13) derived for particle coating. The difference is that  $S$  is now the surface of the web exposed to the precursor.

If again we determine the precursor utilization, we obtain that this is given by the same expression given in Eq. (16)

$$\eta = \frac{1}{1 - \frac{4\phi_0}{v_{th}\beta_0 S} \ln(1 - c)}. \quad (22)$$

As in the case of the particle coating, the precursor efficiency in spatial ALD is determined by the volumetric flow of precursor and the bare reaction probability.

#### E. Universality

We have derived expressions for the throughput and precursor utilization for three different experimental configurations: cross-flow reactor, particle coating, and spatial ALD. The throughput expressions Eqs. (7), (13), and (21) can be unified in a single formula

$$t_c = t_0 + \frac{t_{res}}{\gamma}, \quad (23)$$

where  $t_0$  is the saturation time for a pressure at the entrance of the reactor given by Eq. (14), and represents the fastest possible process, one in which a constant precursor density  $n_0$  is sustained at every point in the reactor during the whole exposure:

$$t_0 = -\frac{4}{\beta_0 s_0 v_{th} n_0} \ln(1 - c). \quad (24)$$

The second term in Eq. (23) is due to the need to transport enough precursor molecules to achieve saturation throughout the reactor. In this term,  $\gamma$  is the so-called excess number, defined as the number of precursor molecules per surface site:<sup>12,15</sup>

$$\gamma = \frac{n_0 s_0 V}{S}. \quad (25)$$

And  $t_{res}$  is the residence time inside the reactor, which is the only variable that depends on the experimental configuration. For the cross-flow case,  $t_{res} = L/u$  is given by the flow velocity and the reactor length, whereas for the particle coating and spatial ALD  $t_{res} = V/\phi$  is given by the volumetric flow and the chamber volume. The physical interpretation of Eq. (23) is simple: reaction and transport take place

simultaneously in the reactor, and the characteristic time will be dominated by the slower process. What changes from configuration to configuration is only the residence time because this depends on the particular reactor design.

In a similar way, we can express the materials utilization as

$$\eta = \frac{1}{1 + \frac{t_0}{t_{\text{res}}}}. \quad (26)$$

Equations (25) and (26) encompass cross-flow, particle coating, and spatial ALD, with  $t_{\text{res}}$  containing the only configuration-specific information. If we now combine both equations, we can extract the relationship between precursor utilization and the minimum dose time required to achieve saturation

$$\eta = 1 - \frac{t_0}{t_c}. \quad (27)$$

Equation (27) establishes a general property of ALD processes: when the process time, or the minimum dose time required for saturation in the system,  $t_c$  is close to the time for saturating an individual site, ( $t_c/t_0 \rightarrow 1$ ) the fraction of precursor actually incorporated into the film tends to zero. In other words, when the throughput is high, the precursor utilization is low. Conversely, when the process is transport limited, ( $t_c/t_0 \gg 1$ ) the precursor utilization is high, but the throughput is low. This trade-off is illustrated in Fig. 6.

One important characteristic of Eq. (27) is that  $t_0$  depends only on the ALD chemistry but not the details of the experimental system. This means that for a known ALD process [i.e., reactive sticking coefficient, vapor pressure, and growth per cycle, see Eq. (24)], we can determine the precursor utilization simply by measuring the minimum time to saturation,  $t_c$ . Alternatively, given two desired values of process time and precursor utilization, we can determine the value of  $t_0$  that would be required

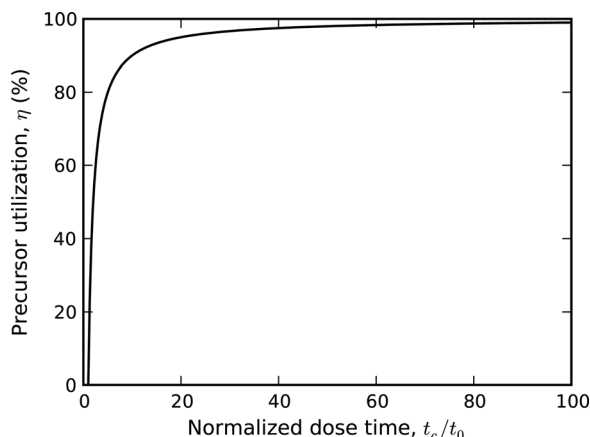


FIG. 6. Interplay between precursor utilization and normalized precursor dose time. This relationship is valid for cross-flow, particle coating, and spatial ALD conditions under the well-mixed reactor approximation. Note that in order to achieve more than 95% precursor utilization dose times at least 50 times larger than the saturation time are required.

$$t_0 = t_c(1 - \eta). \quad (28)$$

Given the expression for  $t_0$  [Eq. (14)], we find that

$$t_c(1 - \eta) \sim \frac{1}{s_0 \beta_0 n_0}. \quad (29)$$

Therefore, in order to achieve both short processing times and high precursor efficiencies, faster ALD kinetics are required. This can be accomplished by increasing the reaction probability, the growth per cycle (which is inversely proportional to the average surface site area,  $s_0$ ), or the precursor vapor pressure. The impact of the product  $\beta_0 s_0 n_0$  on  $t_0$  is shown in Fig. 7 for selected temperature and molecular mass values.

### III. DISCUSSION

In this work, we developed analytic solutions for ALD processes for cross-flow, particle coating, and spatial ALD conditions. These models are based on a first-order, irreversible Langmuir kinetic model that reproduces the main aspects of the ALD chemistry. In the case of the cross-flow reactors, we showed that this simple model agrees well with experimental growth profiles. Therefore, the comparison of axial profiles in cross-flow reactors with the expression given by Eq. (6) can be used as a convenient tool to understand the surface chemistry of new ALD processes. The plug-flow model for cross-flow reactors is based on the following two approximations: (1) The characteristic transverse diffusion time is short compared with the residence time. This is required to ensure that the gas profiles in the reactor are cross-sectionally homogeneous, or at least stationary. (2) Axial diffusion can be neglected when compared with axial advection. In a previous work, we analyzed these requirements for cross-flow reactors.<sup>15</sup> The axial Peclet numbers for a base pressure of 1 Torr and an axial velocity of 1 m/s, the conditions used during the acquisition of the experimental data in Fig. 1, were shown to be larger than one, thus ensuring the validity of the plug-flow approximations.

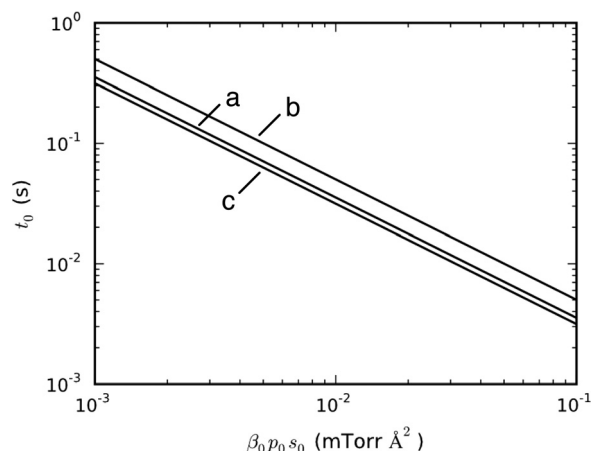


FIG. 7. Impact of the reaction probability  $\beta_0$ , precursor pressure  $p_0$ , and surface site area  $s_0$  on the precursor dose time  $t_0$  for selected conditions, (a)  $T = 473$  K,  $M = 150$  amu; (b)  $T = 473$  K and  $M = 300$  amu; (c)  $T = 373$  K and  $M = 150$  amu. Note that  $t_0$  is a function of the product:  $\beta_0 p_0 s_0$ .

By comparing the expressions for minimum process times and precursor utilization under the three conditions explored in this work, we derived a single formula that captures the interplay between transport and self-limited chemistry in ALD processes. A fourth case not considered yet is transport under purely diffusive conditions, for instance, during the coating of high aspect ratio features. In earlier works,<sup>12,25</sup> we showed how Gordon's expression for the saturation dose time in circular pores<sup>29</sup> could be generalized to the case of arbitrary reaction probability and pore shape using

$$t_c = -\frac{4}{\beta_0 s_0 v_{th} n_0} \ln(1-c) + \frac{L^2 S}{DV n_0 s_0}. \quad (30)$$

Here,  $L$  is the pore length,  $S/V$  is the specific surface area (area per unit volume), and  $D$  is the diffusion coefficient, which can be molecular or Knudsen. In view of the results presented in the previous section, we can now express this equation as

$$t_c = t_0 + \frac{t_{diff}}{\gamma}, \quad (31)$$

where  $t_0$  and  $\gamma$  are defined in the previous section, and  $t_{diff}$  is given by

$$t_{diff} = \frac{L^2}{D}. \quad (32)$$

Therefore, we can see how the universality of Eq. (23) can be expanded to include purely diffusive flow.

It is also important to point out that the expressions derived for particle coating and spatial ALD assume a well-mixed reactor. This constitutes the best-case scenario in which precursor transport in the reactor is fast enough to compensate for precursor consumed in the ALD process. In reality, precursor depletion can further reduce the throughput with respect to the predictions of the well-stirred reactor model, as recently suggested in the literature.<sup>28</sup> The same limitations are present in the cross-flow model, which assumes that the characteristic time for precursor transport to the walls is much faster than the rate of precursor consumption.<sup>15</sup> For situations in which this is not the case, the expres-

sions derived in this work will underestimate the throughput, and full 3-D simulations of the reactors will be required.

One consequence of the analysis in the previous section is that the minimum possible time to achieve saturation for any of the three configurations considered corresponds to  $t_0$ , given by Eq. (14). Thus,  $t_0$  offers the absolute limit for a given ALD process. This minimum time corresponds to the situation in which the precursor injection is high enough to compensate for its depletion and in which the transport takes place instantaneously. Not surprisingly, this time  $t_0$  decreases for higher precursor density. However, it is worth mentioning that the reaction probability,  $\beta_0$ , and the growth per cycle,  $s_0$ , play equally important roles. Therefore, in the search for more efficient ALD precursors, it is important to design not only for high vapor pressure, but also for high reaction probability and growth per cycle. As shown in the previous section, high reaction probabilities also contribute to a higher precursor efficiency. Consequently, the gains in throughput and precursor utilization achieved by a high reaction probability could offset the cost of a more expensive precursor.

Our approach assumes ideal first-order Langmuir behavior, but this assumption can be violated in ALD processes that exhibit non-idealities such as soft saturation, "parasitic" CVD, or surface recombination. However, even in such cases excellent fits to the experimental profiles can be obtained, albeit with increased saturation times compared to the expressions provided in this manuscript. Formally extending the plug flow and well-mixed approximations to include these more complex surface processes is straightforward, but would almost certainly preclude analytic expressions such as those presented above.

Finally, Eq. (6) was obtained under the assumption that the other steps in the ALD cycle were completely saturated, so that coverage profiles are completely determined by only one of the two or more components of a single ALD cycle. Here, we briefly show how this process can be extended to study a sequence of pulses during ALD. The key step is to realize that the final coverage of precursor 1,  $c_{1f}(z)$  is equal to the fraction of available sites of precursor 2,  $\theta_{20}(z)$ . This allows us to express the  $n$ th A/B ALD cycle of the synthesis process as

$$c_{1f}^{(n)}(z) = 1 - \frac{c_{2f}^{(n-1)}(z) \exp\left(\frac{S}{Vu} \frac{1}{4} v_{th}^{(1)} \beta_1 \int_0^z c_{2f}^{(n-1)}(z', 0) dz'\right)}{\exp\left(\frac{S}{Vu} \frac{1}{4} v_{th}^{(1)} \beta_1 \int_0^z c_{2f}^{(n-1)}(z', 0) dz'\right) + \exp\left(s_0 \frac{1}{4} v_{th}^{(1)} \beta_1 \bar{n} t_1\right)} - 1, \quad (33)$$

$$c_{2f}^{(n)}(z) = 1 - \frac{c_{1f}^{(n)}(z) \exp\left(\frac{S}{Vu} \frac{1}{4} v_{th}^{(2)} \beta_2 \int_0^z c_{1f}^{(n)}(z', 0) dz'\right)}{\exp\left(\frac{S}{Vu} \frac{1}{4} v_{th}^{(2)} \beta_2 \int_0^z c_{1f}^{(n)}(z', 0) dz'\right) + \exp\left(s_0 \frac{1}{4} v_{th}^{(2)} \beta_2 \bar{n} t_2\right)} - 1, \quad (34)$$

where  $\beta_1$  and  $\beta_2$  are the reaction probabilities,  $\bar{n}t_1$  and  $\bar{n}t_2$  are the doses, and  $v_{th}^{(1)}$  and  $v_{th}^{(2)}$  are the mean thermal speeds of precursors 1 and 2, respectively. Given the initial coverage conditions, one can calculate the changes in coverage as the number of cycles. In the steady-state regime, we can impose periodic boundary conditions, and assume that  $c_i^{(n-1)}(z) = c_i^{(n)}(z)$  for both precursors. The actual growth per cycle is equal to the difference in coverage before and after a dose,  $GPC = c_1^{(n)}(z) - c_{10}^{(n)}(z) = c_1^{(n)}(z) + c_2^{(n-1)}(z) - 1$ . It is easy to see that Eqs. (33) and (34) reduce to the two asymptotic cases. For sufficiently long pulses  $\bar{n}t_2$ ,  $c_2(z) \rightarrow 1$  in Eq. (34), and Eq. (33) reduces to Eq. (6). Likewise, if  $\bar{n}t_2 = 0$ , then by Eq. (34) we obtain  $c_2^{(n)}(z) = 1 - c_1^{(n)}(z)$ , which gives  $GPC = 0$  during the next cycle. Equation (33) then transforms into an iterative equation whose fixed point is simply that  $c_1(z) \rightarrow 1$ . That is, after multiple cycles of the same precursor, the whole reactor becomes saturated.

#### IV. SUMMARY AND CONCLUSIONS

In this work, we have derived analytic solutions for coverage, throughput, and materials utilization for ALD in three of its most common experimental configurations: cross-flow reactors, particle coating, and spatial ALD conditions. These analyses lead us to unified expressions for throughput and materials utilization valid for all three cases in which the role of reactor design is confined to a single parameter measuring the residence time of unreacted precursor in the reactors. For cross-flow reactors, a comparison with thickness measurements showed that, despite its simplicity, the model can reproduce experimental saturation profiles. Consequently, the analytic model can provide information on the ALD surface chemistry (reaction probability) for new and established ALD processes. Finally, we would like to point out that the expressions derived in this work could be used as a starting point for cost models and feasibility studies to develop manufacturing processes based on atomic layer deposition.

#### ACKNOWLEDGMENTS

A.Y.G. was supported in part by the Argonne-Northwestern Solar Energy Research (ANSER) Center, an Energy Frontier Research Center funded by the U.S. Department of Energy, Office of Science, Office of Basic Energy Sciences under Award Number DE-SC0001059. J.W.E. was supported as part of the Institute for Atom-efficient Chemical Transformations (IACT), an Energy Frontier Research Center funded by the U.S. Department of Energy (DOE), Office of Science, Office of Basic Energy

Science. This work was supported in part by the U.S. Department of Energy, Office of Science, Office of Basic Energy Sciences and Office of High Energy Physics under contract DE-AC02-06CH11357 as part of the Large Area Picosecond Photodetector (LAPPD) project.

- <sup>1</sup>S. Vajda *et al.*, *Nat. Mater.* **8**, 213 (2009).
- <sup>2</sup>J. L. Lu, B. S. Fu, M. C. Kung, G. M. Xiao, J. W. Elam, H. H. Kung, and P. C. Stair, *Science* **335**, 1205 (2012).
- <sup>3</sup>Y. S. Jung, A. S. Cavanagh, A. C. Dillon, M. D. Groner, S. M. George, and S. H. Lee, *J. Electrochem. Soc.* **157**, A75 (2010).
- <sup>4</sup>G. Dingemans and E. Kessels, *J. Vac. Sci. Technol. A* **30**, 040802 (2012).
- <sup>5</sup>G. Agostinelli, A. Delabie, P. Vitanov, Z. Alexieva, H. F. W. Dekkers, S. De Wolf, and G. Beaucarne, *Sol. Energy Mater. Sol. Cells* **90**, 3438 (2006).
- <sup>6</sup>A. A. Dameron, S. D. Davidson, B. B. Burton, P. F. Carcia, R. S. McLean, and S. M. George, *J. Phys. Chem. C* **112**, 4573 (2008).
- <sup>7</sup>P. Poedt, D. C. Cameron, E. Dickey, S. M. George, V. Kuznetsov, G. N. Parsons, F. Roozeboom, G. Sundaram, and A. Vermeer, *J. Vac. Sci. Technol. A* **30**, 010802 (2012).
- <sup>8</sup>J. R. Wank, S. M. George, and A. W. Weimer, *Powder Technol.* **142**, 59 (2004).
- <sup>9</sup>E. Granneman, P. Fischer, D. Pierreux, H. Terhorst, and P. Zagwijn, *Surf. Coat. Technol.* **201**, 8899 (2007).
- <sup>10</sup>J. Dendooven, D. Deduysche, J. Musschoot, R. L. Vanmeirhaeghe, and C. Detavernier, *J. Electrochem. Soc.* **156**, P63 (2009).
- <sup>11</sup>H. C. M. Knoops, E. Langereis, M. C. M. van de Sanden, and W. M. M. Kessels, *J. Electrochem. Soc.* **157**, G241 (2010).
- <sup>12</sup>A. Yanguas-Gil and J. W. Elam, *Chem. Vap. Deposition* **18**, 46 (2012).
- <sup>13</sup>J. W. Elam, D. Routkevitch, P. P. Mardilovich, and S. M. George, *Chem. Mater.* **15**, 3507 (2003).
- <sup>14</sup>M. Ylilammi, *J. Electrochem. Soc.* **142**, 2474 (1995).
- <sup>15</sup>A. Yanguas-Gil and J. W. Elam, *J. Vac. Sci. Technol. A* **30**, 01A159 (2012).
- <sup>16</sup>R. A. Adomaitis, *J. Cryst. Growth* **312**, 1449 (2010).
- <sup>17</sup>A. Holmqvist, T. Torndahl, and S. Stenstrom, *Chem. Eng. Sci.* **81**, 260 (2012).
- <sup>18</sup>W. A. Kimes, E. F. Moore, and J. E. Maslar, *Rev. Sci. Instrum.* **83**, 083106 (2012).
- <sup>19</sup>S. D. Elliott, *Semicond. Sci. Technol.* **27**, 074008 (2012).
- <sup>20</sup>S. D. Elliott and J. C. Greer, *J. Mater. Chem.* **14**, 3246 (2004).
- <sup>21</sup>J. M. Lin, A. V. Teplyakov, and J. C. F. Rodriguez-Reyes, *J. Vac. Sci. Technol. A* **31**, 021401 (2013).
- <sup>22</sup>C. J. Taylor, D. C. Gilmer, D. G. Colombo, G. D. Wilk, S. A. Campbell, J. Roberts, and W. L. Gladfelder, *J. Am. Chem. Soc.* **121**, 5220 (1999).
- <sup>23</sup>S. M. Gates and S. K. Kulkarni, *Appl. Phys. Lett.* **58**, 2963 (1991).
- <sup>24</sup>Y. Yang, S. Jayaraman, D. Y. Kim, G. S. Girolami, and J. R. Abelson, *Chem. Mater.* **18**, 5088 (2006).
- <sup>25</sup>A. Yanguas-Gil and J. W. Elam, in *Atomic Layer Deposition Applications* 7, edited by J. W. Elam, A. Londergan, O. VanDerStraten, F. Roozeboom, S. DeGendt, S. F. Bent, and A. Delabie (Electrochemical Soc Inc., Pennington, 2011), Vol. 41, pp. 169–174.
- <sup>26</sup>H. C. M. Knoops, J. W. Elam, J. A. Libera, and W. M. M. Kessels, *Chem. Mater.* **23**, 2381 (2011).
- <sup>27</sup>D. E. Rosner, *Transport Processes in Chemically Reacting Flow Systems* (Dover, Mineola, New York, 2000).
- <sup>28</sup>P. Poedt, J. van Lieshout, A. Illiberi, R. Knaepen, F. Roozeboom, and A. van Asten, *J. Vac. Sci. Technol. A* **31**, 01A108 (2013).
- <sup>29</sup>R. G. Gordon, D. Hausmann, E. Kim, and J. Shepard, *Chem. Vap. Deposition* **9**, 73 (2003).